Design of Microstrip Bandpass Filters With a Dual-Passband Response

Jen-Tsai Kuo, *Senior Member, IEEE*, Tsung-Hsun Yeh, and Chun-Cheng Yeh

***Abstract*—This paper presents a rigorous design of microstrip bandpass filters with a dual-passband response in parallel-coupled and vertical-stacked configurations. Based on resonance characteristics of a stepped impedance resonator (SIR), the second resonant frequency can be tuned over a wide range by adjusting its structure parameters. Emphasis is placed on filter synthesis for simultaneously matching in-band response and singly loaded Q by using tapped input/output couplings for the two designated passbands. Fractional bandwidth design graphs are used to determine proper geometric parameters of each coupled stage when filter specification is given. Realizable fractional bandwidths of the two passbands for a coupled SIR structure are clearly depicted in fractional bandwidth design graphs. Several experimental filters are fabricated and measured to demonstrate the design.**

***Index Terms*—Dual-passband, microstrip circuit, planar microwave filters, stepped impedance resonator (SIR).**

I. Introduction

RECENT advances in wireless communication have created a need for dual-band operation for RF devices. For example, RF integrated transceivers are fabricated for both global system for mobile communiations (GSM) and wireless code-division multiple-access (WCDMA) purposes [1], [2], dual-band antennas are designed for receiving signals at 0.9/1.8 GHz [3] and at 2.4/5.2 GHz [4], and a dual-frequency rectenna is developed for wireless power transmission [5]. In addition, bandpass filters are realized in monolithic [6] and planar forms [7]–[10]. It is noted that the modules in [1], [2], and [6] consist of two integrated circuits, and each of them is implemented individually for one frequency band. This is a viable alternative using a double diplexing scheme consisting of two distinct filters which are diplexed at each end to achieve the desired two-port dual-band characteristics. In this way, extra impedance-matching networks have to be designed for the two-in and two-out structure [6]. In [9], dual-band bandpass filters are developed by using a cascade of a wide-band bandpass filter and a bandstop filter. Obviously, a single circuit capable of operation in two designated bands will be preferred, since the cost and circuit area can be greatly saved.

It is known that a straight microstrip resonator has resonant frequencies at multiples of its fundamental resonance. It is, of course, not suitable for constructing a dual-frequency filter of which the second frequency is not twice the first one. Thus, the resonators have to be modified. In [7], a lumped capacitor is attached to the center of an open-circuited uniform impedance resonator (UIR). The capacitor will not affect the odd resonances, but it will lower the even-mode frequencies. Therefore, the second frequency of the structure will be limited to be lower than twice the first one. If a stepped impedance resonator (SIR) is employed, on the other hand, both the fundamental and the second resonances can be easily adjusted over a wide frequency range by simply changing its structural parameters [11]. As a result, the second resonance can be either higher or lower than twice the fundamental one. In [8], SIRs are used to successfully design dual-band filters in comb and hairpin structures. Unfortunately, the filter order and description of design method are limited.

Thus far, it is still a real challenge to circuit designers in designing a single filter with two passbands which are simultaneously synthesized. In [10], planar filters with a dual-passband quasi-elliptic function response are presented. Four hairpin resonators with two different geometric dimensions are designed to establish appropriate couplings in the cross-coupled structure.

In this paper, based on SIRs, we describe a rigorous design method for a single filter with a dual-passband response in vertical-stacked and the well-known parallel-coupled configurations. Section II briefly reviews the resonant characteristics of an SIR and discusses how SIR dimensions are adjusted to have resonances at two designated center frequencies of the dual-band response. Section III formulates the design method. Both coupling length and coupling gap of a coupled stage are adjusted at the same time to meet the coupling coefficients required by the two bands. Fractional bandwidth design graphs are provided and their use is explained in detail. These graphs show the possible ranges of geometric parameters of each coupled stage for simultaneous synthesis of the two passbands. In Section IV, simulation and measured results for several experimental filters are presented to validate the design procedure. Section V draws the conclusions.

II. Resonant Characteristics of an SIR

The SIR in Fig. 1 has nonuniformly spaced resonant frequencies, which are roots of the following transcendental equations [11], [12]:

$$\tan\theta_1 = R\cot\theta_2 \quad \text{odd mode} \tag{1}$$

$$\cot\theta_1 = -R\cot\theta_2 \quad \text{even mode} \tag{2}$$

Manuscript received June 27, 2004; revised August 22, 2004. This work was supported by the National Science Council, Taiwan, R.O.C., under Grant NSC 93-2213-E-009-095 and Grant 93-2752-E-009-002-PAE.

J.-T. Kuo and C.-C. Yeh are with the Department of Communication Engineering, National Chiao Tung University, Hsinchu 300, Taiwan, R.O.C. (e-mail: jtkuo@cc.nctu.edu.tw).

T.-H. Yeh was with the Department of Communication Engineering, National Chiao Tung University, Hsinchu 300, Taiwan, R.O.C. He is now with the BENQ Corporation, Hsinchu 300, Taiwan, R.O.C.

Digital Object Identifier 10.1109/TMTT.2005.845765

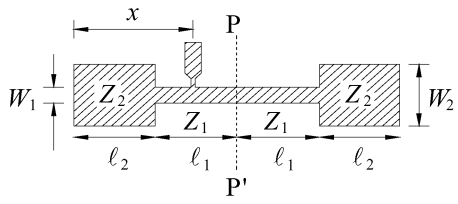

Fig. 1. SIR with input/output tapping.

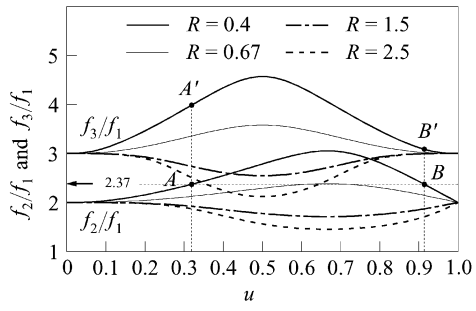

Fig. 2. Normalized f_2/f_1 and f_3/f_1 for an SIR with impedance ratios $R = 0.4, 0.67, 1.5$, and 2.5. $u = \theta_2/(\theta_1 + \theta_2)$.

where θ_1 and θ_2 are electrical lengths of the microstrip sections with characteristic impedances Z_1 and Z_2, respectively, and $R = Z_2/Z_1$ is the impedance ratio of the SIR. These two equations can be formulated by setting the plane of symmetry P–P' to be short- and open-circuited for the odd and even resonances, respectively. The fundamental and consecutive higher order resonances of the SIR occur alternatively in odd and even modes.

Based on the solutions to (1) and (2), Fig. 2 shows the second (f_2) and third (f_3) resonant frequencies normalized with respect to the first one (f_1) for $R = 0.4, 0.67, 1.5$, and 2.5. The variable of the horizontal axis u, called the length ratio, is defined as

$$u = \frac{\theta_2}{\theta_1 + \theta_2}. \tag{3}$$

The plots in Fig. 2 provide proper u and R values to realize the designated f_2/f_1 ratio. Fig. 2 clearly shows that, the smaller R is, the larger the maximum ratio of f_2/f_1 is. If $f_2 \geq 2f_1$ is required, $R \leq 1$ should be chosen, and vice versa. Also, away from the plateau or valley of any of the curves, one can see that there are always two possible u values for a given R to obtain the same f_2/f_1 ratio. The u value corresponding to the larger f_3/f_1 is preferred, since it corresponds a wider upper rejection band. For example, if the two passbands are at 2.45 and 5.8 GHz, i.e., $f_2/f_1 = 2.37$, and $R = 0.4$ is used, then $u = 0.317$ at point A is better than that at B, since the ratio f_3/f_1 at A' is larger than that at B'.

III. Fractional Bandwidth Design Graph

Next, we determine the coupling scheme of each pair of adjacent SIRs to meet the required coupling coefficients for two respective bands. When two resonators have a close proximity,

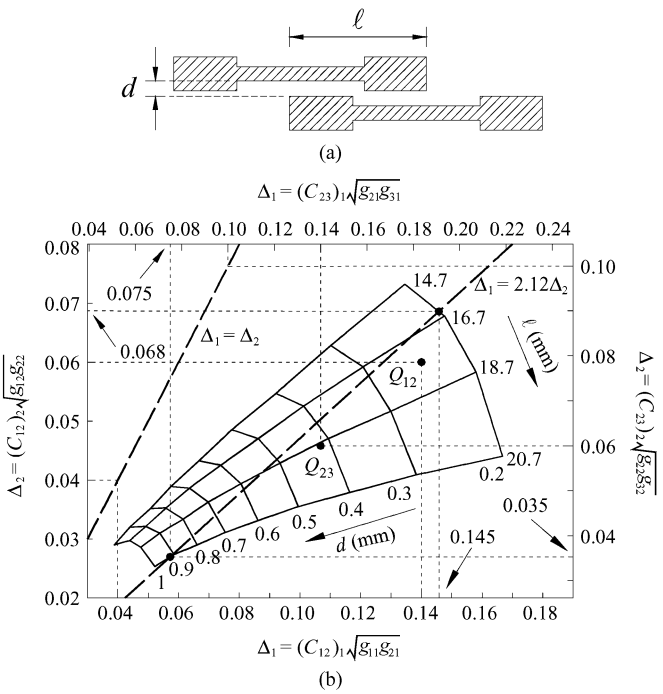

Fig. 3. (a) Coupling structure. (b) Fractional bandwidth design graph. $f_1 = 2.45$ GHz, $f_2 = 5.2$ GHz. Dimensions of SIR in mm: $W_1 = 0.89, W_2 = 1.30, \ell_1 = 11.38, \ell_2 = 9.32$. Substrate: $\varepsilon_r = 2.2$, thickness $= 0.508$ mm.

the coupling coefficient C and their resonant frequencies are related by [11]

$$C = \frac{f_a^2 - f_b^2}{f_a^2 + f_b^2} \tag{4}$$

where f_a and f_b are peak frequencies in the transmission response obtained by using excitation through a gap to the outer ends of the coupled resonators. There are N resonators in an Nth-order filter. In our filter design, the coupling coefficients between the nth and $(n+1)$th resonators have also to be specified by element values g_{nk} and $g_{n+1,k}$ of the low-pass filter prototype and fractional bandwidth Δ_k as [13]

$$(C_{n,n+1})_k = \frac{\Delta_k}{\omega_1' \sqrt{g_{nk} g_{n+1,k}}} \tag{5}$$

where ω_1' is the cutoff frequency of the low-pass filter prototype, and the subscript $k = 1$ or 2 denotes the first or the second passband. Note that (4) should be evaluated around two designated center frequencies to meet the use of (5).

A. Parallel-Coupled Filters With Tapped Input/Output

Taking the advantage of structural symmetry, we design Chebyshev filters only of odd orders for this configuration. For example, a fifth-order Chebyshev filter with tapped input/output has $(C_{12})_k = (C_{45})_k$ and $(C_{23})_k = (C_{34})_k$. For a coupled stage in Fig. 3(a), let the coupling length be ℓ and the coupling gap be d. In conventional design of a bandpass filter with a single passband, the coupling length ℓ is usually half of that of an entire resonator, e.g., [11]. In fact, both ℓ and d can be tuned in certain respective ranges to provide the same coupling coefficient. In other words, there are two degrees of freedom in

designing a coupled stage. Thus, it is possible to make a coupled stage match the two coefficients required by specifications of two passbands.

The coupling length and gap of a coupled stage in Fig. 3(a) have to provide two proper coupling coefficients at two designated frequencies. This can be done by constructing a fractional bandwidth design graph shown in Fig. 3(b) as follows. Let the design frequencies be at 2.45 and 5.2 GHz and both passbands have 0.1-dB ripple levels. Given $\ell(\text{mm}) = 14.7, 16.7, 18.7$, and 20.7, and $d(\text{mm}) = 0.2, 0.3, \ldots, 1$, the coupling coefficients of the coupled SIRs are evaluated by (4) using the EM simulation package IE3D.[1] Note that the coupling coefficient in (5) is proportional to the fractional bandwidth, since the element values of the low-pass filter prototype are constants when filter order and ripple level are specified. Thus, the coordinates of fractional bandwidth design graphs for this coupling structure associated with filter specification are then obtained. It is worth mentioning that the right vertical axis can be obtained from the left one by just multiplying a constant $[(g_{22}g_{32})/(g_{12}g_{22})]^{1/2}$, and the upper axis can be scaled from the lower one in a similar fashion.

The use of Fig. 3(b) can be explained as follows. First, note that, for all possible d and ℓ values given in Fig. 3(b), possible Δ_1 is between 0.04 and 0.17, and possible Δ_2 is less than 0.075. If $\Delta_1 = 0.14$ and $\Delta_2 = 0.06$ are chosen, one can locate a point Q_{12} with $\ell = 17.7$ mm and $d = 0.25$ mm for $(C_{12})_k$ and $(C_{45})_k$, and locate a point Q_{23} with $\ell = 18.7$ mm and $d = 0.42$ mm for $(C_{23})_k$ and $(C_{34})_k$. It is beneficial to know the feasible bandwidths for the filter specification before the circuit is designed. This can be done by drawing a straight line of $\Delta_1/\Delta_2 =$ constant with the graph. For example, when $\Delta_1/\Delta_2 = 1$, the dashed line clearly indicates that there is no solution within the given ranges of ℓ and d for designing a dual-passband response. However, when $\Delta_1/\Delta_2 = 5.2/2.45 = 2.12$, i.e., both passbands have identical absolute bandwidths, realizable Δ_1 is from 0.075 (upper axis) to 0.145 (lower axis) and Δ_2 is from 0.035 (right axis) to 0.068 (left axis), as indicated. It is noted that, when the SIR geometries or the design frequencies are changed, the design graphs should be recalculated.

Fig. 3(b) is also useful for design of a third-order Chebyshev filter. Again, we have $(C_{12})_k = (C_{23})_k$. The horizontal axis $(C_{12})_1$ of the design graphs is that of Fig. 3(b) scaled by multiplying $[(g_{11}g_{21})_{\text{order}=3}/(g_{11}g_{21})_{\text{order}=5}]^{1/2}$, and the vertical axis $(C_{12})_2$ can be obtained in the same way.

B. Vertical-Stacked Filters

We are also interested in designing vertical-stacked SIR filters with a dual-passband response. One of the important features of this filter is its compact area [14]. Two basic coupling structures A and B involved in circuit design are shown in Fig. 4(a). Based on these two couplings, the filter can be designed in two possible configurations. One starts with coupling A and the other with B. Let's call the former filter type $\boldsymbol{A}$ and the latter type $\boldsymbol{B}$. In a vertical-stacked filter of order n, structures A and B occur alternatively. For example, schematic layouts for such fourth-order filters of types $\boldsymbol{A}$ and $\boldsymbol{B}$ are given in Fig. 4(b). For a filter of type $\boldsymbol{A}$, only $C_{12} = C_{34}$ and C_{23} need establishing by structures A and B, respectively.

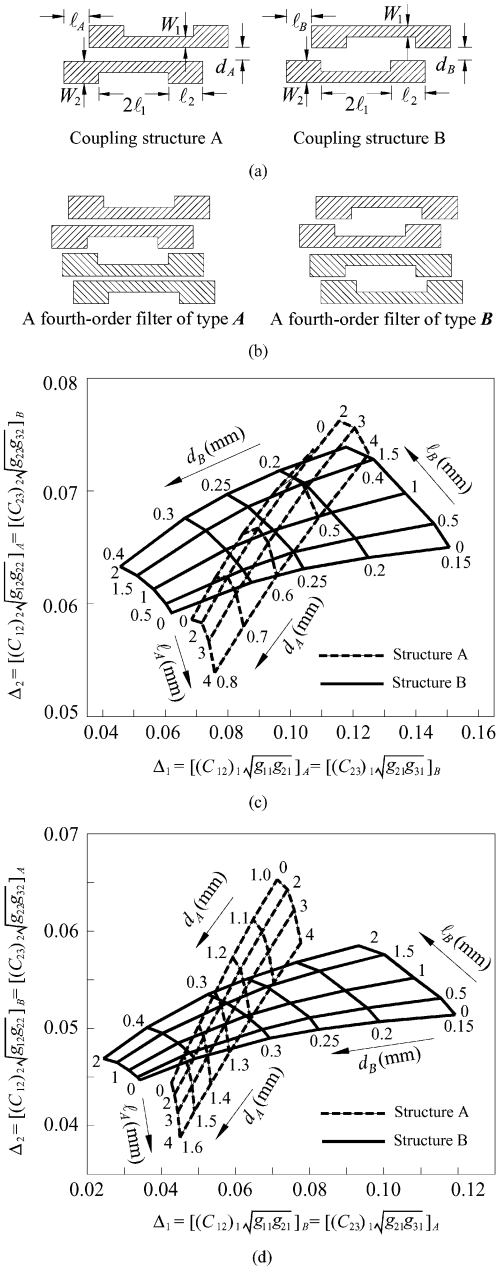

Fig. 4. Structures and design graphs for vertical-stacked SIR filters. (a) Coupling structures. (b) Schematic layouts for fourth-order filters of types $\boldsymbol{A}$ and $\boldsymbol{B}$. (c) Fractional bandwidth design graphs for filter type $\boldsymbol{A}$. (d) Design graphs for filter type $\boldsymbol{B}$. $f_1 = 2.45$ GHz and $f_2 = 5.8$ GHz. Dimensions of SIR in mm: $W_1 = 0.46, W_2 = 1.11, \ell_1 = \ell_2 = 9.47$. Substrate: $\varepsilon_r = 2.2, \text{thickness} = 0.508$ mm.

Fig. 4(c) plots the design graphs for filter type $\boldsymbol{A}$. The SIR has $f_1 = 2.45$ GHz, $f_2 = 5.8$ GHz, $u = 0.5, Z_1 = 100\ \Omega$, and $Z_2 = 62.7\ \Omega$. The coordinates are based on a fourth-order Chebyshev response with a ripple level of 0.1 dB. For both the horizontal and vertical axes of Fig. 4(c), the corresponding Δ_1 and Δ_2 are enforced identical after $(C_{12})_{1,2}$ of coupling structure A and $(C_{23})_{1,2}$ of B are multiplied by the square root of the product of element values of the low-pass filter prototype.

[1]IE3D Simulator, Zeland Software Inc., Freemont, CA, Jan. 1997.

Similarly, the design graphs in Fig. 4(d) are for vertical-stacked filters of type ***B***. It is worth mentioning that the design graphs in Fig. 4(c) and (d) are originated from the same coupling coefficients obtained by (4). The two sets of graphs look different since the coefficients are multiplied by different constants to form the respective horizontal and vertical axes. The significance of plotting Fig. 4(d) is twofold. First, the overlap areas of the graphs in Fig. 4(c) and (d) consist of possible solutions to filter type ***A*** and type ***B***, respectively. Second, for coupling structure A, the range of required gap sizes in Fig. 4(c) is much different from that in Fig. 4(d).

C. Design Filters of Higher Orders

The concept in Fig. 3 can be extended to design parallel-coupled filters of higher orders. If a seventh-order filter is designed, one more horizontal axis $\Delta_1 = (C_{34})_1(g_{31}g_{41})^{1/2}$ and one more vertical axis $\Delta_2 = (C_{34})_2(g_{32}g_{42})^{1/2}$ can be added to Fig. 3. In this case, the scales of all axes in Fig. 3 should be changed since the element values of the seventh-order low-pass filter prototype are different from those of a fifth-order one. More axes can be used for synthesizing filters of further increased orders.

It is important to note that the realizable Δ_1 and Δ_2 should be the common region of all horizontal and vertical axes, respectively. Obviously, the higher the filter order is, the smaller the realizable regions of Δ_1 and Δ_2 will be. In addition, any change of passband specification will cause element values of the low-pass filter prototype to vary, and the feasible ranges of Δ_1 and Δ_2 will change accordingly.

The same idea applies to design of higher order filters of the vertical-stacked configuration.

D. Input/Output Tapping

Tapped-line input is applied to the end resonators. The singly loaded $Q(Q_{si})$ of a tapped resonator is calculated as [15]

$$Q_{si} = \frac{R_L\omega_0}{2}\left.\frac{\partial B(\omega)}{\partial\omega}\right|_{\omega=\omega_0} \tag{6}$$

where R_L is the load impedance seen at the tap point by the resonator looking to the load and $B(\omega)$ is the total susceptance of the resonator seen at the tap point. Obviously, Q_{si} in (6) is a function of x and should be evaluated at the two designated frequencies. Let

$$(Q_{si})_k = R_{Lk}N_k(x) \tag{7}$$

where the expression of $N_k(x)$ can be derived as in [11]. It is known that Q_{si} should also be specified by [13]

$$(Q_{si})_k = \frac{\omega_1' g_{0k}g_{1k}}{\Delta_k}. \tag{8}$$

Now, we have to make the tapped point x in Fig. 1 satisfy $(Q_{si})_1$ and $(Q_{si})_2$ at both frequencies. Substituting (7) into (8), one can obtain the ratio

$$\frac{\Delta_1}{\Delta_2} = \frac{R_{L2}N_2(x)}{R_{L1}N_1(x)}\frac{g_{01}g_{11}}{g_{02}g_{12}}. \tag{9}$$

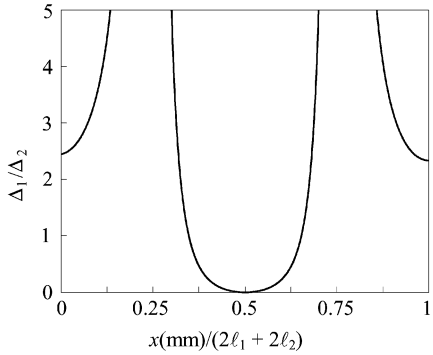

Fig. 5. Ratio Δ_1/Δ_2 versus the tap position (see Fig. 1). SIR dimensions are in Fig. 3. Total length of the SIR is $2\ell_1 + 2\ell_2 = 41.38$ mm.

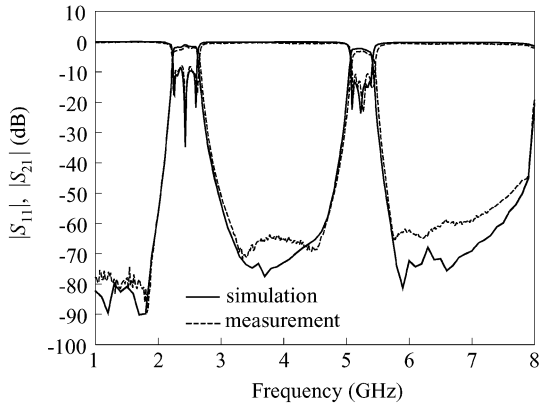

Fig. 6. Simulation and measured responses of a fifth-order Chebyshev filter. $f_1 = 2.45$ GHz, $f_2 = 5.2$ GHz, $\Delta_1 = 14\%$, $\Delta_2 = 6\%$. Dimensions of the SIRs are given in Fig. 3.

For $R_{L1}g_{01}g_{11} = R_{L2}g_{02}g_{12}$, Fig. 5 plots Δ_1/Δ_2 against x for the SIR in Fig. 3. It is clear from the plot that, once Δ_1/Δ_2 is specified, the tap position can be easily located. Again, if the SIR structure is changed, this plot should be changed accordingly. The load impedances R_{L1} and R_{L2} can be different, and their ratio can be a tunable parameter for the design. For convenience, $R_{L1} = R_{L2}$ is used. In this case, the dual-frequency transformer [16] can be employed.

IV. Simulation and Measured Filter Responses

Three parallel-coupled filters in Figs. 6–8 and two vertical-stacked filters in Figs. 9 and 10 are designed and fabricated to demonstrate the design. Fig. 6 plots the responses of a fifth-order Chebyshev filter with fractional bandwidths $\Delta_1 = 14\%$ and $\Delta_2 = 6\%$. The coupling length and gap size for the first and second SIRs are $\ell_{12} = 17.7$ mm and $d_{12} = 0.24$ mm, and those for the second and third SIRs are $\ell_{23} = 18.7$ mm and $d_{23} = 0.41$ mm, respectively. By letting $R_{L1} = R_{L2}$, the tap position x can be found to be 13.4 mm. Substituting this x value into (5), one can obtain the load impedances $R_{L1} = R_{L2} = 110\,\Omega$. As shown in Fig. 6, the measured responses have a good agreement with the simulated results obtained by the IE3D. In measurements, the insertion losses are -1.7 dB and -2.9 dB at the centers of the first and second passbands, respectively. Note that the geometric parameters of each coupled stage are determined based on the design graph in Fig. 3, thus both the

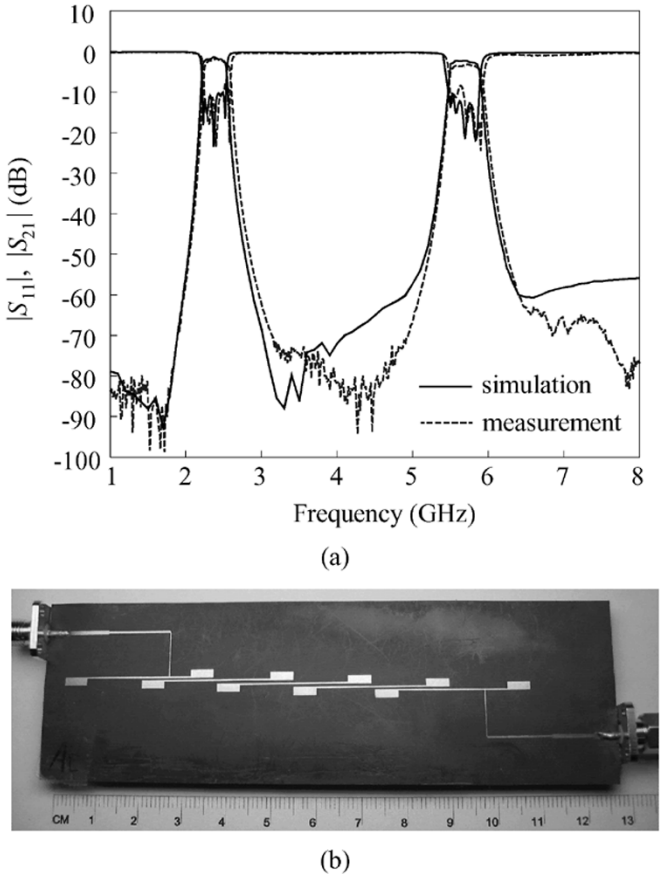

Fig. 7. (a) Simulation and measured responses of a fifth-order Chebyshev filter. $f_1 = 2.45$ GHz, $f_2 = 5.8$ GHz, $\Delta_1 = 12\%, \Delta_2 = 7\%$. Dimensions of SIR in mm: $W_1 = 0.34, W_2 = 1.86, \ell_1 = 11.76, \ell_2 = 5.04$. (b) Photograph of the filter. Substrate $\varepsilon_r = 2.2, \text{thickness} = 0.508$ mm.

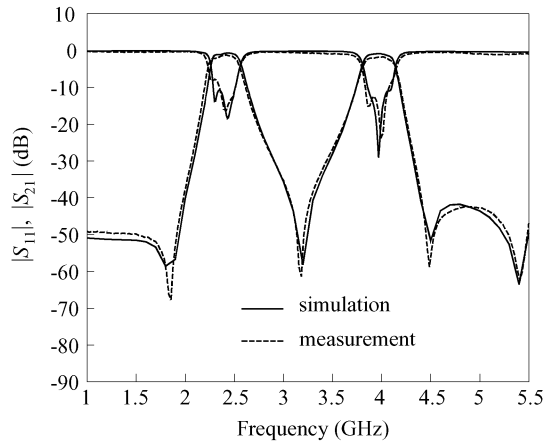

Fig. 8. Simulation and measured results for a third-order filter. $f_1 = 2.45$ GHz, $f_2 = 4.0$ GHz, $\Delta_1 = 6.5\%, \Delta_2 = 4.5\%$. Dimensions of the SIR in mm: $W_1 = 1.55, W_2 = 0.43, \ell_1 = \ell_2 = 13.85, x = 20.01$. Substrate $\varepsilon_r = 2.2, \text{thickness} = 0.508$ mm.

simulation and experimental characteristics of the entire filter shown in Fig. 6 validate the design procedure in Section III.

The $|S_{11}|$ levels at the centers of the two passbands are better than -20 dB, but the maximal magnitudes over the passbands are about -10 dB. This could be resulted from the fact that the dual-frequency transformer has insufficient bandwidths at the

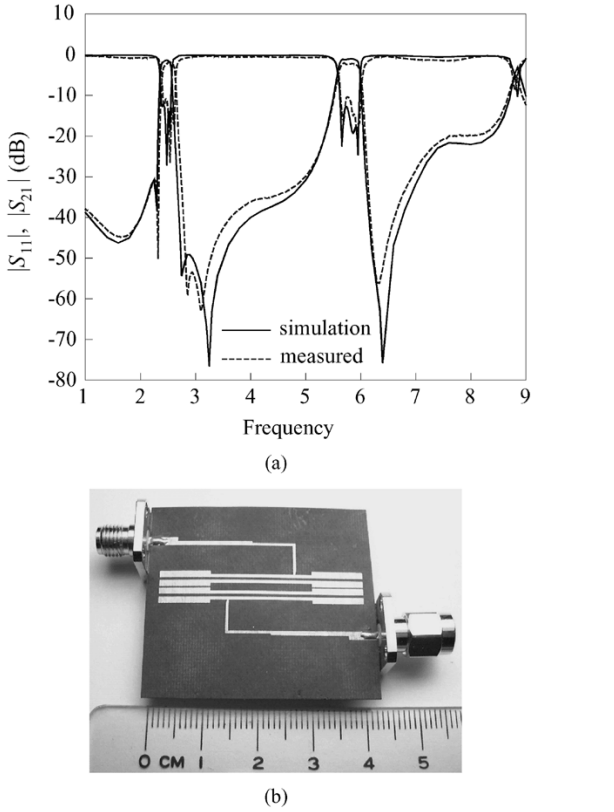

Fig. 9. (a) Simulation and measured responses of a fourth-order stacked-line filter of type $\boldsymbol{A}$. $f_1 = 2.45$ GHz, $f_2 = 5.8$ GHz, $\Delta_1 = 7.2\%, \Delta_2 = 6.0\%$. Dimensions of the SIRs are in Fig. 4. Tap position $x = 12.7$ mm. (b) Photograph of the filter.

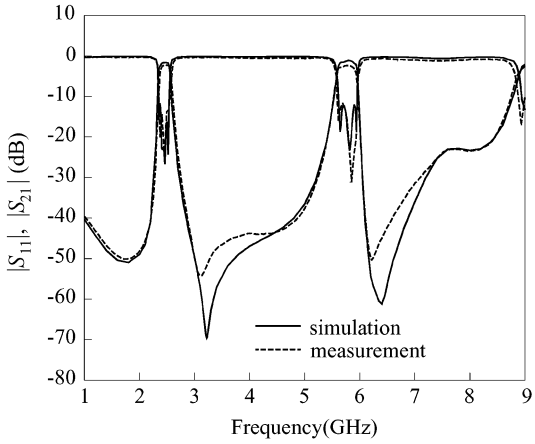

Fig. 10. Simulation and measurement results for a fourth-order vertical-stacked filter of type $\boldsymbol{B}$. $f_1 = 2.45$ GHz, $f_2 = 5.8$ GHz, $\Delta_1 = 7.0\%$, $\Delta_2 = 5.5\%$. Dimensions of the SIRs are given in Fig. 4.

two matching frequencies. We try to improve this by making the impedance levels at the two frequencies different and redesigning the impedance-matching network by modifying the method in [16]. The results show that, if the performance in one band is improved, then the performance of the other deteriorates at the same time. One possible way to resolve this problem could be to use a dual-band impedance transformer with three or more sections.

Fig. 7(a) plots the responses of a fifth-order filter having $f_1 = 2.45$ GHz, $f_2 = 5.8$ GHz, $\Delta_1 = 12\%$, and $\Delta_2 = 7\%$. Dimensions of the fabricated circuit determined by the design graph are $\ell_{12} = 16, \ell_{23} = 16.8, d_{12} = 0.43, d_{23} = 0.6$, and the tap position $x = 9.9$, all in millimeters. In the measured results, the insertion losses are -1.8 and -3.0 dB for the first and second bands, respectively. Fig. 7(b) is a photograph of the filter.

Fig. 8 plots the results of a third-order Chebyshev filter with a passband ripple of 0.01 dB. This filter has $f_1 = 2.45$ GHz, $f_2 = 4.0$ GHz, $\Delta_1 = 6.5\%$, and $\Delta_2 = 4.5\%$. Note that f_2 is less than $2f_1$, so that Z_1Z_2 should be used. The simulated and measured responses are in good agreement. The measured insertion losses are -1.2 and -1.65 dB at the centers of the first and second passbands, respectively.

Fig. 9 plots simulation and measured responses of a fourth-order vertical-stacked filter based on the graphs in Fig. 4(c). It is interesting to note that it is possible to design a bandpass filter with a dual-passband response with $\ell_A = \ell_B = 0$, i.e., all the four SIRs are upright stacked. One can find that there is a unique solution in Fig. 4(c), where the fractional bandwidths for the first and second passbands are 7.2% and 6.0%, respectively, and the corresponding gap sizes are $d_A = 0.65$ mm and $d_B = 0.36$ mm. The measured passband insertion losses are -1.8 dB and -2.0 dB for the first and the second bands, respectively. Fig. 9(b) shows a photograph of the circuit.

Fig. 10 plots the responses of a fourth-order vertical-stacked filter of type $\boldsymbol{B}$ using the design graphs in Fig. 4(c). If $\ell_A = \ell_B = 0$ are chosen, the filter will have 4.5% fractional bandwidths. This is not easy for microstrip implementation. We then turn to choose $\Delta_1 = 7.0\%$ and $\Delta_2 = 5.5\%$. Important geometric parameters are $d_A = 1.1, d_B = 0.24, \ell_A = 4$, and $\ell_B = 1.6$, all in millimeters. The measured passband insertion losses are -2.2 and -2.4 dB for the first and second bands, respectively.

V. Conclusion

This paper presents a detailed procedure for design of parallel-coupled and vertical-stacked microstrip filters with a dual-passband response. By using SIRs with a fundamental resonance at $f_1 = 2.45$ GHz, the second frequency f_2 can be either larger or smaller than $2f_1$ by trimming its dimensions. The design fully utilizes both coupling length and coupling gap of a coupled stage to meet the two different coupling coefficients for the dual-band purpose. In this study, third- and fifth-order parallel-coupled filters with $f_2 = 4.0, 5.2$, and 5.8 GHz are demonstrated. Two fourth-order vertical-stacked filters are also designed and measured. Fractional bandwidth design graphs are key reference data for the successful design, since they provide feasible fractional bandwidths for the two designated bands. The design procedure also applies to design filters of higher orders. The measured responses of the fabricated filters not only have satisfactory responses, but also have good agreement with the simulation results.

Acknowledgment

The authors are grateful to the anonymous reviewers for their positive comments, which have enhanced the readability of this paper.

References

[1] S. Wu and B. Razavi, "A 900-MHz/1.8-GHz CMOS receiver for dual-band applications," *IEEE J. Solid-State Circuits*, vol. 33, no. 12, pp. 2178–2185, Dec. 1998.

[2] J. Ryynänen, K. Kivekäs, J. Jussila, A. Pärssinen, and K. A. I. Halonen, "A dual-band RF front-end for WCDMA and GSM applications," *IEEE J. Solid-State Circuits*, vol. 36, no. 8, pp. 1198–1204, Aug. 2001.

[3] D. Llorens, P. Otero, and C. Camacho-Penalosa, "Dual-band, single CPW port, planar-slot antenna," *IEEE Trans. Antennas Propagat.*, vol. 51, no. 1, pp. 137–139, Jan. 2003.

[4] Y.-L. Kuo and K.-L. Wong, "Printed double-T monopole antenna for 2.4/5.2 GHz dual-band WLAN operations," *IEEE Trans. Antennas Propagat.*, vol. 51, no. 9, pp. 2187–2192, Sep. 2003.

[5] Y.-H. Suh and K. Chang, "A high-efficiency dual-frequency rectenna for 2.45- and 5.8-GHz wireless power transmission," *IEEE Trans. Microw. Theory Tech.*, vol. 50, no. 7, pp. 1784–1789, Jul. 2002.

[6] H. Miyake, S. Kitazawa, T. Ishizaki, T. Yamada, and Y. Nagatomi, "A miniaturized monolithic dual band filter using ceramic lamination technique for dual mode portable telephones," *IEEE MTT-S Int. Microwave Symp. Dig.*, pp. 789–792, 1997.

[7] K. Wada and O. Hashimoto, "Fundamentals of open-ended resonators and their application to microwave filters," *IEICE Trans. Electron.*, vol. E83-C, pp. 1763–1775, Nov. 2000.

[8] S.-F. Chang, J.-L. Chen, and S.-C. Chang, "New dual-band bandpass filters with step-impedance resonators in comb and hairpin structures," in *Asia–Pacific Microwave Conf.*, 2003, pp. 793–796.

[9] L.-C. Tsai and C. W. Hsue, "Dual-band bandpass filters using equal-length coupled-serial-shunted lines and Z-transform technique," *IEEE Trans. Microw. Theory Tech.*, vol. 52, no. 4, pp. 1111–1117, Apr. 2004.

[10] J.-T. Kuo and H.-S. Cheng, "Design of quasi-elliptic function filters with a dual-passband response," *IEEE Microw. Compon. Lett.*, vol. 14, no. 10, pp. 472–474, Oct 2004.

[11] J.-T. Kuo and E. Shih, "Microstrip stepped impedance resonator bandpass filter with an extended optimal rejection bandwidth," *IEEE Trans. Microw. Theory Tech.*, vol. 51, no. 5, pp. 1554–1559, May 2003.

[12] M. Makimoto and S. Yamashita, "Bandpass filters using parallel coupled stripline stepped impedance resonators," *IEEE Trans. Microw. Theory Tech.*, vol. MTT-28, no. 12, pp. 1413–1417, Dec. 1980.

[13] G. L. Mattaei, L. Young, and E. M. T. Jones, *Microwave Filters, Impedance-Matching Network, and Coupling Structures*. Norwood, MA: Artech House, 1980.

[14] E. Shih and J.-T. Kuo, "A new compact microstrip stacked-SIR bandpass filters with transmission zeros," in *IEEE MTT-S Int. Microwave Symp. Dig.*, 2003, pp. 1077–1080.

[15] J. S. Wong, "Microstrip tapped-line filter design," *IEEE Trans. Microw. Theory Tech.*, vol. MTT-27, no. 1, pp. 44–50, Jan. 1979.

[16] C. Monzon, "A small dual-frequency transformer in two sections," *IEEE Trans. Microw. Theory Tech.*, vol. 51, no. 4, pp. 1157–1161, Apr. 2003.

Jen-Tsai Kuo (S'88–M'92–SM'04) received the Ph.D. degree from the Institute of Electronics, National Chiao Tung University (NCTU), Hsinchu, Taiwan, R.O.C., in 1992.

Since 1984, he has been with the Department of Communication Engineering, NCTU. During 1995, he was a Visiting Scholar with the University of California at Los Angeles. He is currently a Professor with the Department of Communication Engineering, NCTU, and serves as the Chairman of the Degree Program of the College of Electrical Engineering and Computer Science. His research interests include the analysis and design of high-frequency electronics and microwave active and passive circuits, high-speed interconnects and packages, field-theoretical studies of guided waves, and numerical techniques in electromagnetics.

Tsung-Hsun Yeh was born in Taichung, Taiwan, R.O.C., on March 14, 1979. He received the B.S. degree in electrical and control engineering and M.S. degree in communication engineering from the National Chiao Tung University, Hsinchu, Taiwan, R.O.C., in 2001 and 2003, respectively.

His research interests include the design of microwave active and passive circuits. He is currently an RF Engineer with the BENQ Corporation, Hsinchu, Taiwan, R.O.C.

Chun-Cheng Yeh was born in Chiayi, Taiwan, R.O.C., on June 25, 1980. He received the B.S. degree in electrical engineering from the National Sun Yat-Sen University, Kaohsiung, Taiwan, R.O.C., in 2002, and the M.S. degree in communication engineering from the National Chiao Tung University, Hsinchu, Taiwan, R.O.C., in 2004.

His research interests include the design of microwave planar filters and RF modules for microwave and millimeter-wave applications.